Arab J Sci Eng (2015) 40:1579–1590
DOI 10.1007/s13369-015-1625-x

RESEARCH ARTICLE - CIVIL ENGINEERING

Effect of Bridge Pier Position on Scour Reduction According to Flow Direction

Adnan Ismael · Mustafa Gunal · Hamid Hussein

Received: 24 February 2014 / Accepted: 1 March 2015 / Published online: 15 March 2015

Abstract An experimental approach was conducted to study the effect of the change in the position of bridge pier on scour reduction with respect to flow direction. The experiments included the study of new method to reduce scour depth in front of bridge pier by changing the position of bridge pier (named after here as downstream facing round-nosed bridge pier). The down flow deflected away from the front of the opposite pier, and the vortex becomes small and does not affect the pier. In this study, three piers—circular 10 cm, upstream facing round-nosed (10–4) cm and downstream facing round-nosed (4–10) cm bridge piers—were tested under live-bed condition with flow intensity of 58 l/s for duration of 3 h. The velocity field measurements were obtained using an Acoustic Doppler Velocimeter. The results showed that the downstream facing round-nosed pier reduces local scour. The reduction in maximum scour depth was 54 % when compared to the circular pier and 40 % compared with upstream facing round-nosed pier. The downstream facing round-nosed pier reduces local scour by a volume of 83 % when compared to the circular pier. Changing the position of bridge pier (as is located downstream facing to the flow) is an effective countermeasure for reducing local scour depth. Empirical relationship was developed on the basis of obtained results. The present experimental study shows that there is no need of any alteration or modification to countermeasure scour like riprap, collar and slot. The present method also reduces costs and improves the hydraulic performance of bridge pier.

Keywords Experimental study · Bridge pier position · Opposite pier · Scour reduction · Local scour

List of symbols

b	Pier width (m)
v	Flow velocity (m/s)
ρ	Density of fluid (kg/m^3)
h	Flow depth (m)
g	Gravitational acceleration (m/s^2)
d_{50}	Median particle size (mm)
k_s	Shape factor= $\frac{D_{u/s}}{Dd/s}$
$D_{u/s}$	Upstream diameter of pier (m)
$D_{d/s}$	Downstream diameter of pier (m)
D	Pier diameter (m)
Fr	Froude number = $\left[\frac{v}{\sqrt{gh}}\right]$
F_{D50}	Densimetric Froude number
R	Correlation coefficient
d_{16}	Grain size for which 16 % by weight of the sediment is finer
d_{84}	Grain size for which 84 % by weight of the sediment is finer
$\partial g = (d_{84}/d_{16})^{0.5}$	Geometric standard deviation of the grain size distribution

1 Introduction

The local scour along a river is defined as the removal of bed material around an obstacle immersed in a flow field. If the obstacle is a bridge pier, the biggest danger is repre-

A. Ismael · M. Gunal (✉)
Civil Engineering, Gaziantep University, Gaziantep, Turkey
e-mail: gunal@gantep.edu.tr

H. Hussein
Technical College, Mosul, Iraq
e-mail: Dr.hamid22a@yahoo.com

A. Ismael
Technical Institute, Mosul, Iraq
e-mail: adnan_esmaeel@yahoo.com

sented by the possible undermine of piers foundations that can take to bridge's collapse. During the past decades, several investigations were conducted to assess the adequacy of countermeasures against local scour at bridge piers. The shape of the bridge piers has important effect on the local scour. Therefore, different shapes of bridge piers should be investigated experimentally and numerically to find a reliable efficiency before field application, especially under live-bed scour condition.

The present study is perhaps the first experimental work to place bridge pier in opposite direction according to flow direction under live-bed condition as shown in Fig. 1.

Reduction in scour around bridge piers has been studied by many researchers [1–4] experimentally and numerically. These researches are focused on reducing local scour around the bridge pier by constructing countermeasures around pier. Existing literature revealed that the shape of the obstruction to the flow can strongly affect the flow pattern around it and the strength of the down flow, horseshoe vortex and the wake vortex are greater in the case of square piers compared to circular piers. Few studies have been reported on the local scour around non-circular piers such as round-nosed piers. The round-nosed pier reduces the bed shear stress value more than a circular pier does [5]. Two bridge pier shapes (circular and round-nosed) were chosen in the present study to compare the depth of local scour. Round-nosed-shape bridge pier is located in two different ways: upstream and downstream facing Fig. 1. The present experimental study showed that local scour around downstream facing round-nosed pier reduced 54 and 40 % comparing with circular and upstream facing round-nosed piers. Although the local scour reduced significantly, manufacturing of the round-nosed bridge pier is

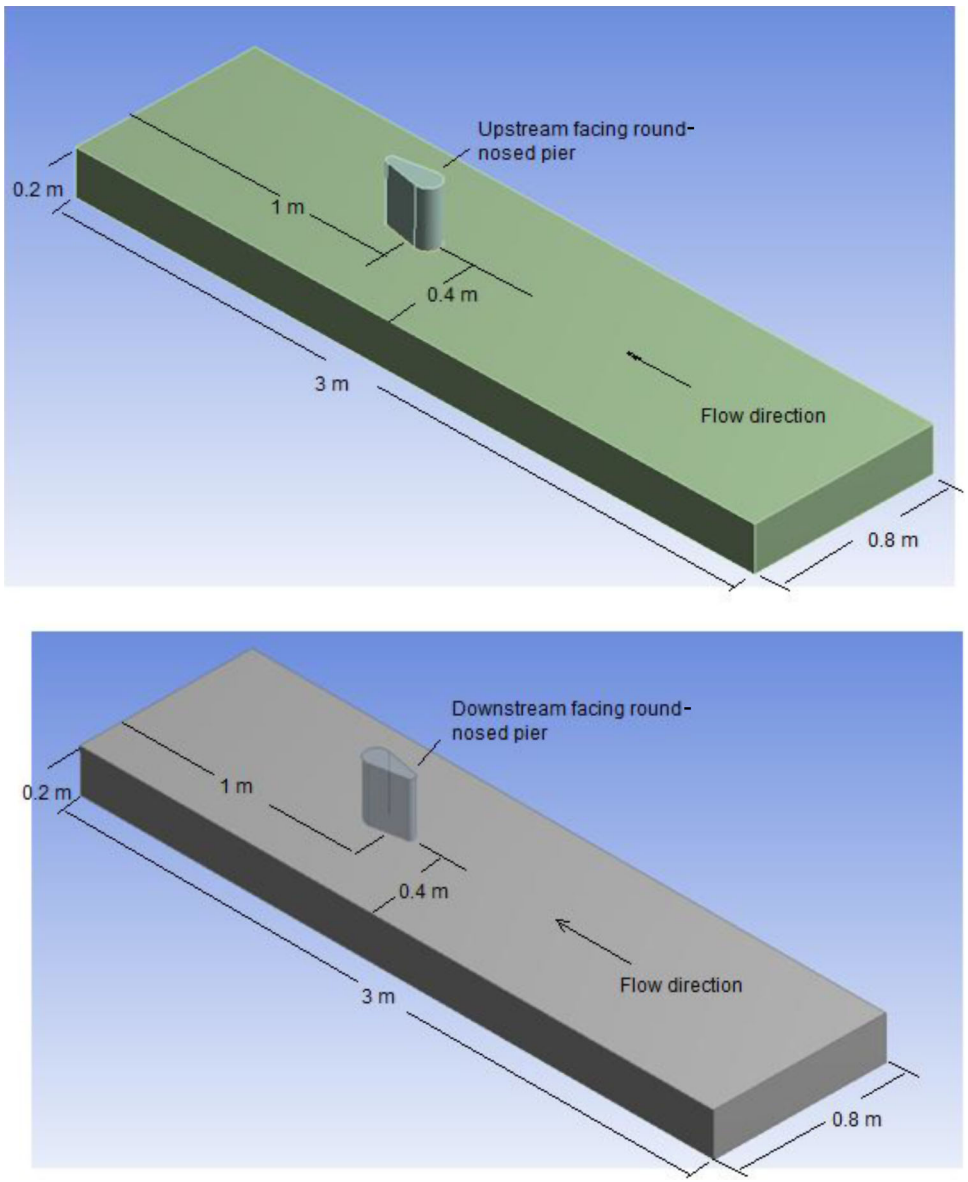

Fig. 1 Location of upstream and downstream round-nosed bridge pier to the flow direction

time-consuming when compared with that of the circular pier. Therefore, designers do not prefer to use any shapes different than circular. But there are many examples of bridge piers having same upstream and downstream nose diameter. Our study investigates the performance of different upstream and downstream round nose diameter with respect to local scour and compares the experimental results with the most practically used circular piers. The present experimental study shows that round-nosed bridge pier performance is improved by locating it as downstream facing to the flow. We hope that the results of the present study will be benefitted by the designers and engineers.

Scour countermeasures can be basically divided into two groups: armoring countermeasures and flow-altering countermeasures. The main idea behind flow-altering countermeasures is to minimize the strength of the down flow and subsequently horseshoe vortexes, which are the main causes of pier scour. In contrast, the principle of armoring countermeasures is to provide a protection layer that acts as a resistant layer to hydraulic shear stress and therefore provides protection to the more erodible materials underneath. A comprehensive review of flow-altering countermeasures by Tafarojnoruz et al. [6] shows that although several types of flow-altering countermeasures were already investigated and proposed in the literature, some of them exhibit low efficiency in terms of scour depth reduction or suffer from serious problems for practical purposes.

It has been long established that the basic mechanism causing local scour at bridge piers is the down flow at the upstream face of the pier and subsequent formation of vortices at the base of the pier [7].

The performance of six different types of flow-altering countermeasures against pier scour was evaluated experimentally [8]. They found some countermeasures, which were recommended as highly efficient in the literature, do not perform well under test conditions.

Use of a hooked collar for reducing local scour around a bridge pier was examined by Chen et al. [9]. The efficiency of collars was studied through experiments and compared with an unprotected pier. The velocity field measurements were obtained using an Acoustic Doppler Velocimeter. Results showed that a hooked-collar diameter of 1.25b has effectiveness similar to a collar diameter of 4.0b where b is the pier width. With hooked collar installed at the bed level, there was no sign of scouring and horseshoe vortex at the upstream face of the pier. In contrast, with unprotected pier, the down flow and turbulent kinetic energy were reduced under the effects of the hooked collar.

The scour hole characteristics around a single vertical pier in clear water was investigated experimentally by Khwairakpam et al. [10]. They observed that the entire scour geometry (scour depth, length, width, area and volume) depended upon densimetric Froude number (F_{D50}) and inflow depth (h). Empirical relationships were developed on the basis of the obtained results.

Roughness elements with different sizes and spacing as a hydrodynamic countermeasure for local pier scour were utilized [11]. Placement of roughness elements on the perimeter of piers increased the resistance to the down flow and consequently reduced depth of scour hole upstream of the pier up to 30 %.

The modeling work of [12] considered the bed deformation and flow simulation around hydraulic structure. The model uses an improved formula for the bed shear stress by applying vorticity effect and solves the full three-dimensional Reynolds-averaged Navier–Stokes equation to calculate the flow field. The new sedimentation formula takes into account vortices that effect the local scour process. The model was verified by applying the ordinary bed shear stress equation and the improved equation. Comparisons show that the new equation could predict the scour more accurately than the ordinary one.

Flow patterns around a T-shape spur dike and support structure have been simulated by Vaghefi et al. [13]. They used Flow-3D model; the numerical and experimental data are compared in longitudinal section to verify numerical model. The results show very good correspondence between numerical and laboratory data. The support structure has been installed at the upstream of the T-shape spur dike to alter flow patterns and hydraulic parameters, such as power of secondary flow, and separate zone in all sections. The power of secondary flow around main spur dike decreases by 40–120 %, and the length of separation zone increases from 0.8 to 2.5 times bigger than the length of T-shape spur dike.

Tuna and Emiroglu [14] analyze the effect of step geometry on the dynamics of local scour processes in the context of scour that takes place downstream from a stepped chute. Three different step heights have been used to study the scour process for various chute angles, stilling basin sill heights, tailwater depth and flow rate conditions. The results show that the equilibrium depth of scour is highly dependent on the step geometry. In addition, the equilibrium depth of scour decreases while the step height increases. Also, the equilibrium depth of scour also increases with an increase in a discharge and chute angle.

Onen [15] Predict the local scour at a side weir known as a lateral intake structure, which is widely used in irrigation. The study presents artificial neural network (ANN) and gene expression programming (GEP) models, which is an algorithm based on a genetic algorithms and genetic programming, for prediction of the clear-water scour depth at side weir. The GEP-based formulation and ANN approach are compared with laboratory results, multiple linear/nonlinear regression (MLR/MNLR). The performance of GEP is found in slightly more influential than ANN approach and MNLR for predicting the clear-water scour depth at side weir.

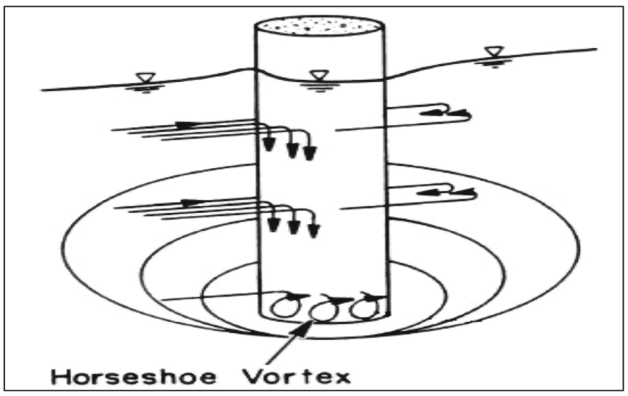

Fig. 2 The horseshoe vortex is created at the upstream side of the pier and wraps around it [8]

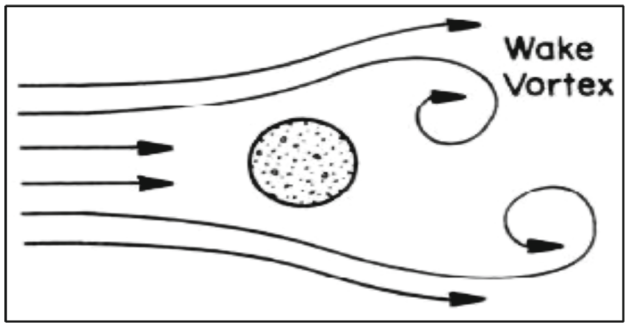

Fig. 3 Wake vortices are formed at the surface of the pier and continue downstream

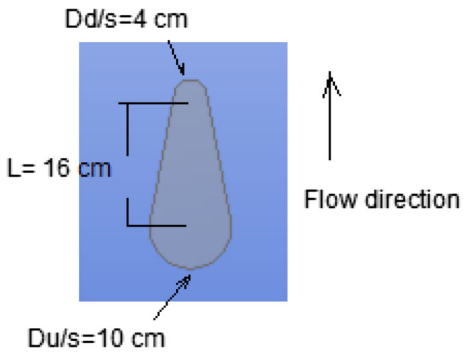

Fig. 4 Dimension of bridge pier

This study concentrated on reducing local scour around bridge piers, by using different upstream and downstream round nose diameters. There are many experimental studies [6,8,16,17] focusing on countermeasures to reduce local scour by flow alteration and armoring methods. Despite the countermeasures, methods are efficient in scour reduction around bridge piers; they need alteration or modification to countermeasure scour like riprap, collar and slot. The present method is an effective countermeasure to reduce the depth of scour and also reduces maintenance costs and improves the hydraulic performance of bridge pier.

2 Local Scour

Local scour around bridge piers is the result of acceleration of the flow and formation of vortices around the piers. As the flow is interrupted, a strong pressure field decreasing with the depth is formed in front of the obstruction. If the pressure field is strong enough, it causes a three-dimensional separation of the boundary layer. It drives the approaching flow downwards, and a recirculating primary vortex is formed on the upstream side of the pier. As the flow passes by the bridge, the vortices wrap around the sides of the piers in the shape of a horseshoe and continue downstream Fig. 2. This is called a horseshoe vortex [18].

The primary vortex system in front of the pier is the main scour force, and it removes bed material from the base of the pier. Since the rate at which material is carried away from the area is greater than the transport rate into it, a scour hole is formed around the pier.

As the scour hole gets deeper, the strength of the vortices at the base of the pier decreases and eventually a state of equilibrium is reached. For a clear-water situation that happens when the shear stress from the vortices equals the critical stress for the sediment particles, and no more bed material is scoured. For a live-bed situation, equilibrium is reached when the amount of sediment inflow equals the amount of outflow from the scour hole. In that situation, the scour depth fluctuates but the average depth remains constant.

Table 1 Experimental data

v (m/s)	h (m)	d_{50}/h	Fr
0.58	0.125	0.0116	0.523
0.54	0.11	0.0132	0.525
0.49	0.096	0.0151	0.51

The horseshoe vortices act mainly on the upstream face and the sides of a pier, whereas on the downstream side of the pier another type of vortices dominates, called wake vortices. They are formed along the surface of the pier, then detached from both sides and continue downstream Fig. 3. The wake vortices together with the accelerated side flow and the upward flow behind the pier cause the downstream scouring. The wake vortices are generated by the pier itself, and their size and strength depend mainly on the velocity of the flow and the pier size and shape. The strength of a wake vortex declines rapidly downstream of a pier, and therefore, there is often a deposit of material downstream of piers [19].

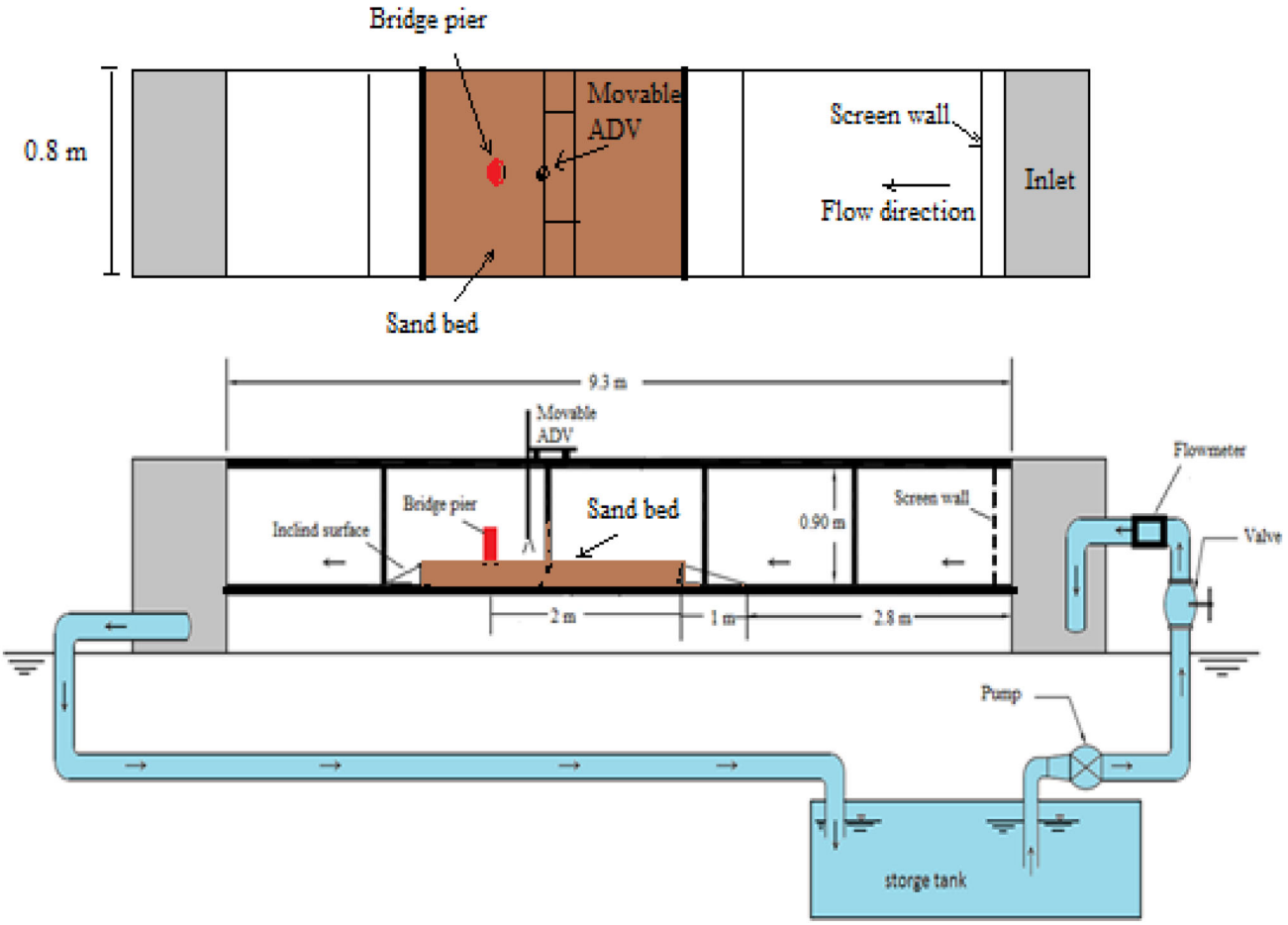

Fig. 5 Schematic layout of the flume

Fig. 6 Grain size distributions

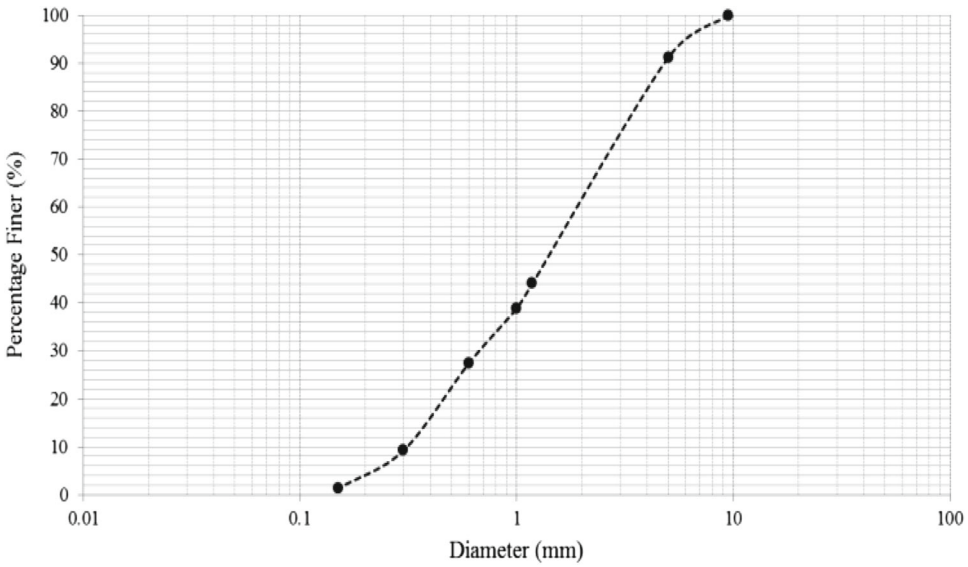

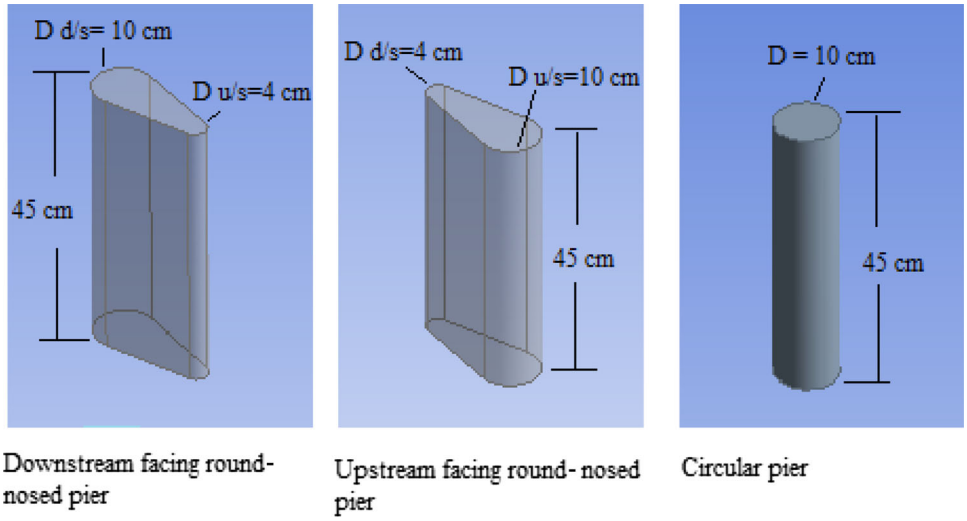

Fig. 7 Three tested bridge piers

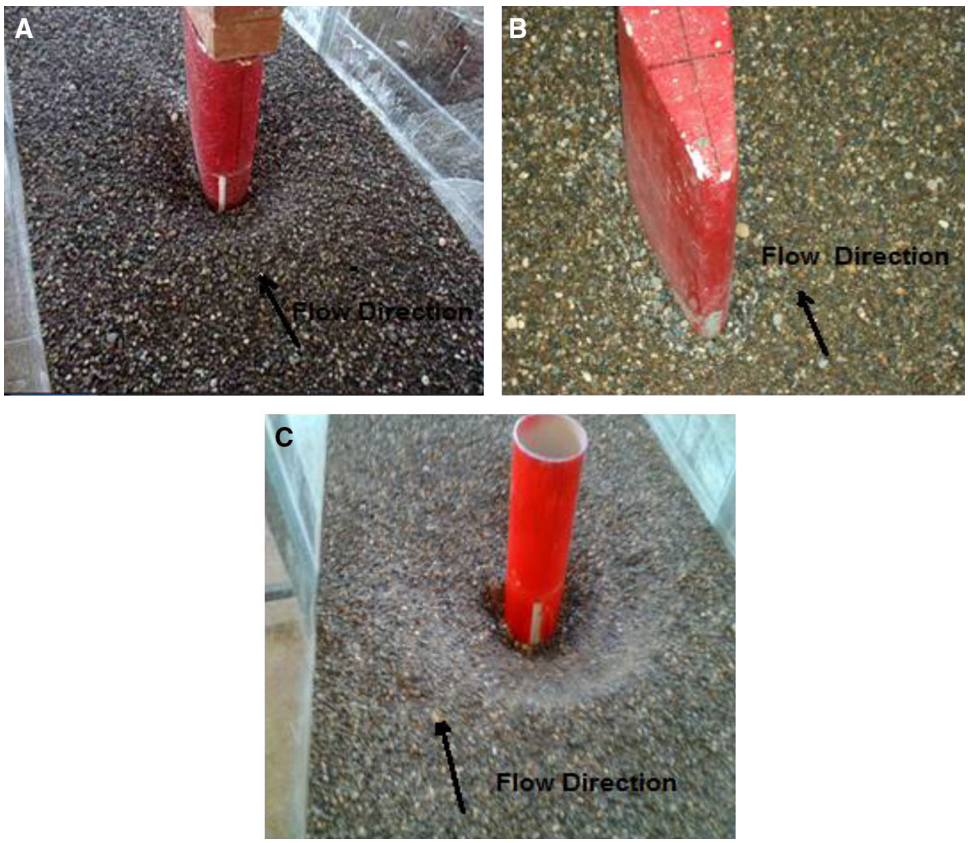

Fig. 8 Scour hole around. **a** Upstream facing round-nosed, **b** downstream facing round-nosed and **c** circular piers

3 Dimensional Analysis

Dimensional analysis was used to define the dimensionless parameters based on the selection of all variables governing the maximum scour depth at upstream of the bridge pier.

$$ds = f_1(v, \rho, h, g, d_{50}, k_s) \tag{1}$$

in which v is the flow velocity, ρ is the density of fluid, h is the flow depth, g is the gravitational acceleration, d_{50} is the median particle size, and k_s is the pier shape factor, which is equal to (1,2.5 and 0.4) for circular, upstream facing round-nosed and downstream facing round-nosed piers, respectively. $k_s = \frac{D_{u/s}}{D_{d/s}}$ shown in Fig. 4.

The maximum relative depth of scour was assumed to be correlated with the other independent parameters as given by Eq. (2).

$$ds/h = f_2\left(Fr, \frac{d_{50}}{h}, k_s\right). \tag{2}$$

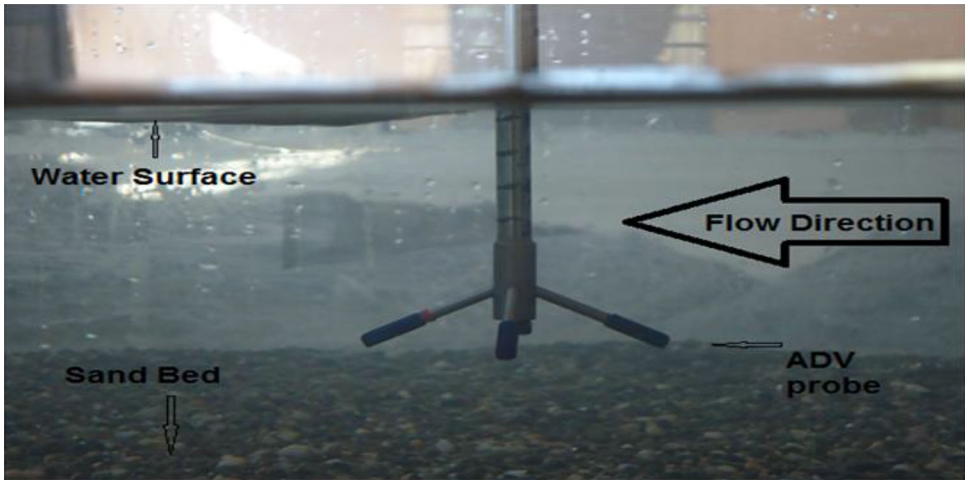

Fig. 9 Typical ADV Setup

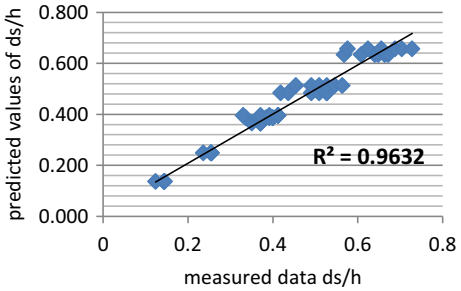

Fig. 10 Measured ds/h versus predicted ds/h

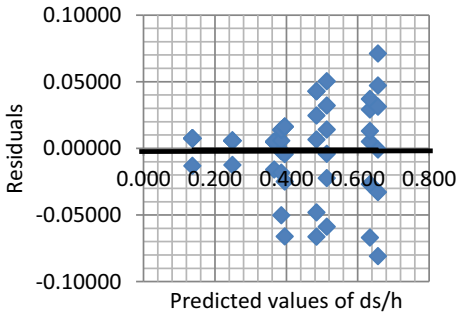

Fig. 11 Predicted ds/h from Eq. 3 versus residual

ds = maximum depth of scour, Fr = Froude number range, and $\frac{d_{50}}{h}$ are listed in Table 1.

4 Experimental Work

The experiments were carried out in the hydraulic laboratory of Civil Engineering Department of Gaziantep University. The flume is 12 m long, 0.8 m wide and 0.9 m deep as shown in Fig. 3 with glass sides and steel bottom.

The test section was made with a ramp which is located at the beginning and the end of the section. The test section is 3 m long and 0.2 m deep as shown in Fig. 5.

Table 2 Scour hole dimensions from physical modeling

Scour hole dimensions	Downstream facing round-nosed bridge pier Diameter = 4–10 cm	Upstream facing round-nosed bridge pier Diameter = 10–4 cm	Circular bridge pier Diameter = 10 cm
Top scour hole width (cm)	30	36	50
Distance from upstream face to front outer edge of hole (cm)	7.0	16	18
Depth at upstream face (cm)	5.0	8.4	10.9

The test section was filled with sediment of median particle size $d_{50} = 1.45$ mm and standard deviation, $\sigma_g = 3.16$ with the specific gravity of 2.65; the sieve analysis of the sand is given in Fig. 6.

Flume discharge was measured by a magnetic flow meter installed in the pipe system before the inlet of channel. The scour hole and the elevation of the bed were measured by laser meter, the instrument mounted on a manually moving carriage sliding on rails on the top of the flume wall. Three piers downstream facing round-nosed, upstream facing round-nosed and circular piers as shown in Fig. 7 were tested.

Experiments were performed under a live-bed water scour regime. The discharge was measured as 58 l/s with 12.5 cm flow depth. Initial bed elevations were taken randomly to check the leveling of the test section by using laser meter. The flume was first filled with water until desirable flow depth to avoid undesirable scour. Inlet flow to the flume was then gradually increased until the desired discharge and the temporal variation of scour were monitored. The scour depth was measured under an intense light. The progress of scour depth was

Table 3 Depth of scour from physical modeling

Time (min)	Discharge (l/s)	Depth of scour for circular pıer (cm)	Depth of scour for upstream facing round-nosed pıer (10–4 cm)	Depth of scour for downstream facing round-nosed pıer (4–10 cm)
5	58	8.6	7.1	4.2
15		9.2	7.5	4.6
30		9.8	8.0	4.8
60		10.2	8.1	4.9
120		10.4	8.3	5.0
180		10.9	8.4	5.0
5	48	6.0	4.6	2.6
15		6.4	4.8	2.8
30		6.8	5.4	2.8
60		6.9	5.6	2.8
120		7.0	5.8	2.8
180		7.0	5.8	2.8
5	38	4.2	3.4	1.2
15		4.6	3.6	1.4
30		5.0	3.6	1.4
60		5.2	3.6	1.4
120		5.3	3.6	1.4
180		5.3	3.6	1.4

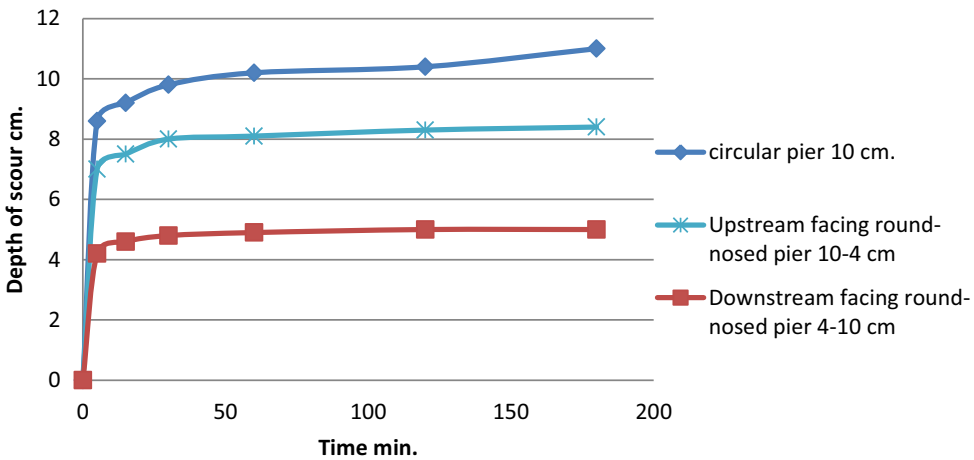

Fig. 12 Scour hole development measured at the upstream face of each tested pier

observed 3 h for three bridge piers as given in Fig. 8. At the end of each test, the pump was shut down and the water was slowly drained without disturbing the scour topography. The test section was then allowed to dry and frozen by pouring glue material (varnish).

5 Acoustic Doppler Velocimeter Measurements

During each experiment, the velocity is periodically monitored using an Acoustic Doppler Velocimeter (ADV). Stream velocity is measured upstream of the pier using the ADV in the center of the flume. The typical ADV setup is shown in Fig. 9.

The ADV probe was then positioned above the scour hole, and velocities were recorded for a period of 180 s. The sample period of 180 s was chosen to ensure that sufficient flow variations were captured.

6 Prediction of Scour Depth

Using stepwise regression (linear + interaction method), Eq. (3) was developed to correlate the relative maximum scour

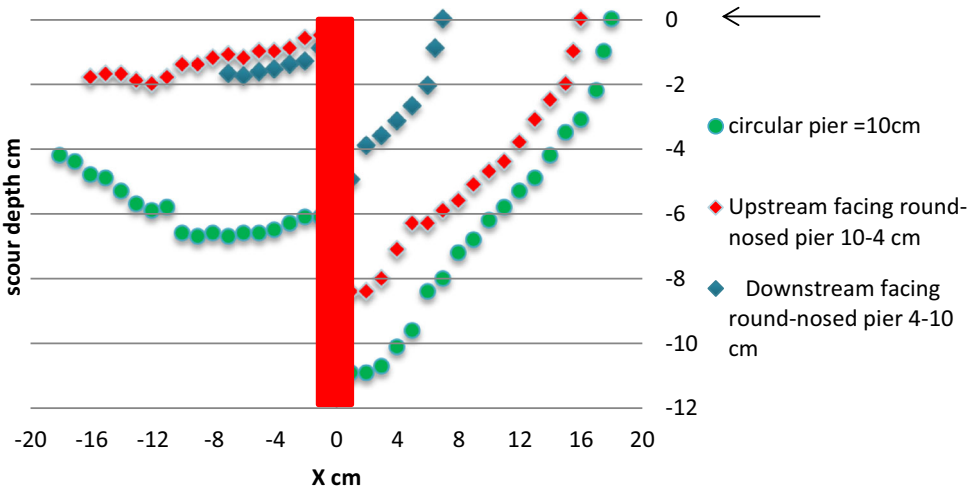

Fig. 13 Longitudinal scours holes of three bridge piers

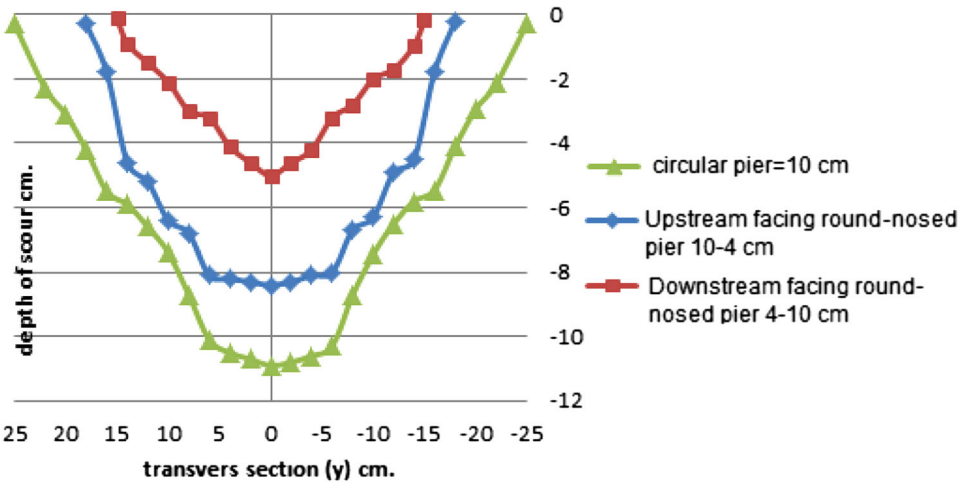

Fig. 14 Transverse scour holes of three bridge piers

depth with the Froude number, Fr, and the pier shape factor, k_s

$$ds/h = 1680.6(d_{50}/h)Fr - 0.121\ln k_s \log(d_{50}/h) - 0.0393k_s^2 e^{Fr} - 1.73 \quad (3)$$

The correlation coefficient (R^2) and the standard error of estimate for Eq. (3) are 96.3 % and 0.032, respectively. Figure 10 presents the predicted values of ds/h using Eq. (3) versus the measured ones, while Fig. 11 shows the distribution of the residuals around the line of zero error. Both figures indicate that Eq. (3) represented the measured data very well and hence could be used safely to predict the relative maximum depth of scour for different shape of piers.

7 Results and Discussion

7.1 Scour Hole Dimensions

Dimensions of the scour holes for each run of experiments were measured. The top width of scour in the transverse direction, distance from upstream face to front outer edge of hole and depth at upstream face were compared for each of the three bridge piers as shown Table 2.

The results of elapsed time taken from the start of each experiment for the scour hole to develop for three piers are given in Table 3.

Experimental results of the model piers within cohesion less bedding material will be compared and discussed in this section. The results are a comparison of scour and sediment scour hole depths for the circular and upstream facing round-nosed piers were quite similar as expected, due to the identical shape on the upstream side of the pier as illustrated in Fig. 12. A 54 % reduction in scour hole depth of the downstream facing round-nosed pier was observed as compared to the circular pier and 40 % reduction as compared to the upstream facing round-nosed pier.

In addition to a reduction of the scour depth, the rate of scouring is also reduced considerably as in Fig. 12. Reduction in the rate of scouring can reduce the risk of pier failure when the duration of floods is short [20].

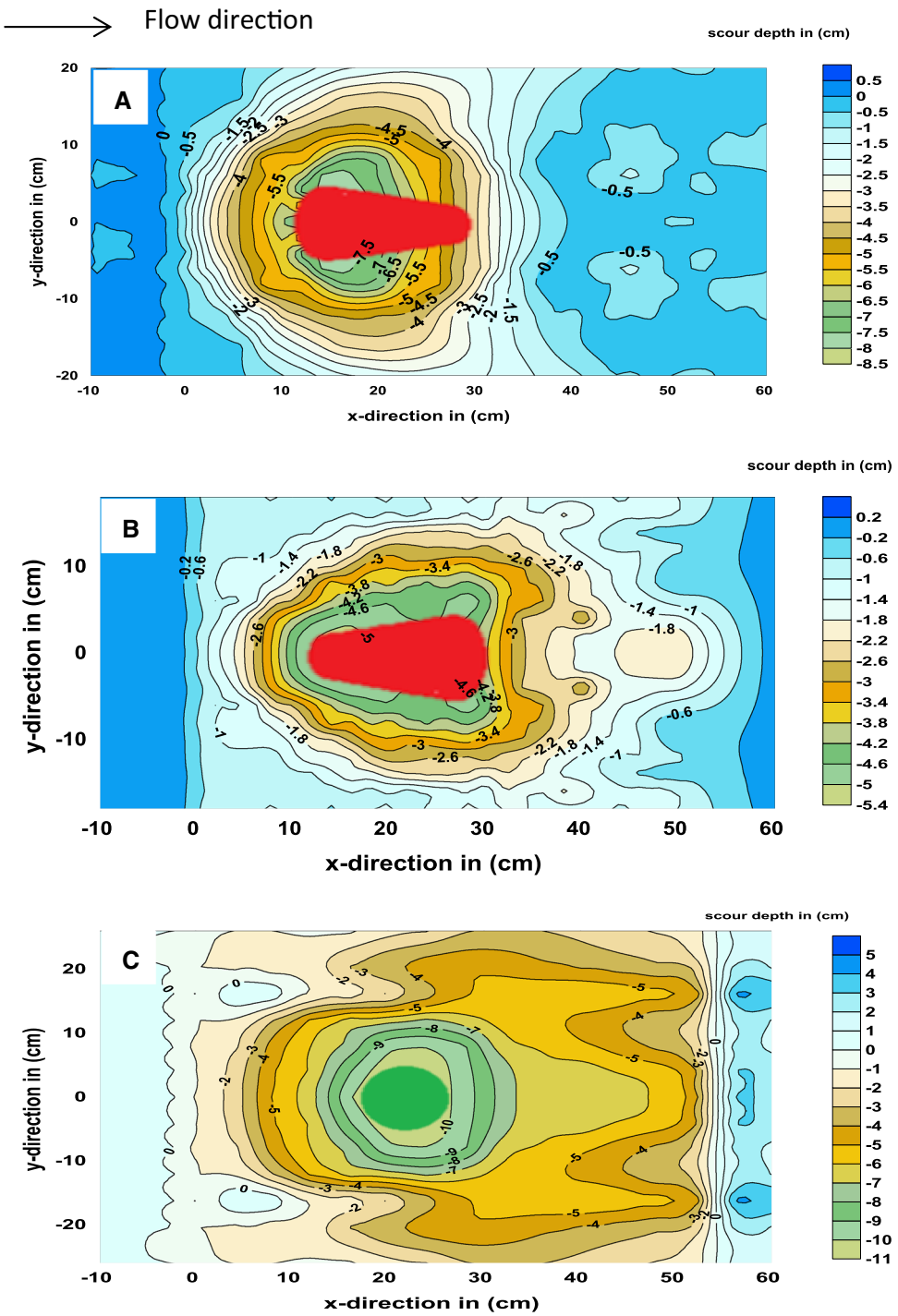

Fig. 15 The scour pattern around. **a** Upstream facing round-nosed, **b** downstream facing round-nosed and **c** circular piers

The percentage reduction in distance from the upstream face of the pier to the upstream front outer edge of the hole as compared to the circular pier was 11 and 61 % for the upstream facing round-nosed and downstream facing round-nosed bridge piers, respectively, as illustrated in Fig. 13.

Figure 14 demonstrates the top scour holes of three bridge piers. The top scour hole width of downstream facing round-nosed pier was 20 cm or 40 % less than the circular pier and 6.0 cm or 17 % less than the upstream facing round-nosed pier because the effect of the horseshoe vortex was reduced due to the down flow being deflected away from the base of opposite pier.

Figure 15 shows the scour pattern around the upstream facing round-nosed, downstream facing round-nosed and circular piers. The downstream facing round-nosed pier minimizes the scour depth, producing a little scour in the front and on

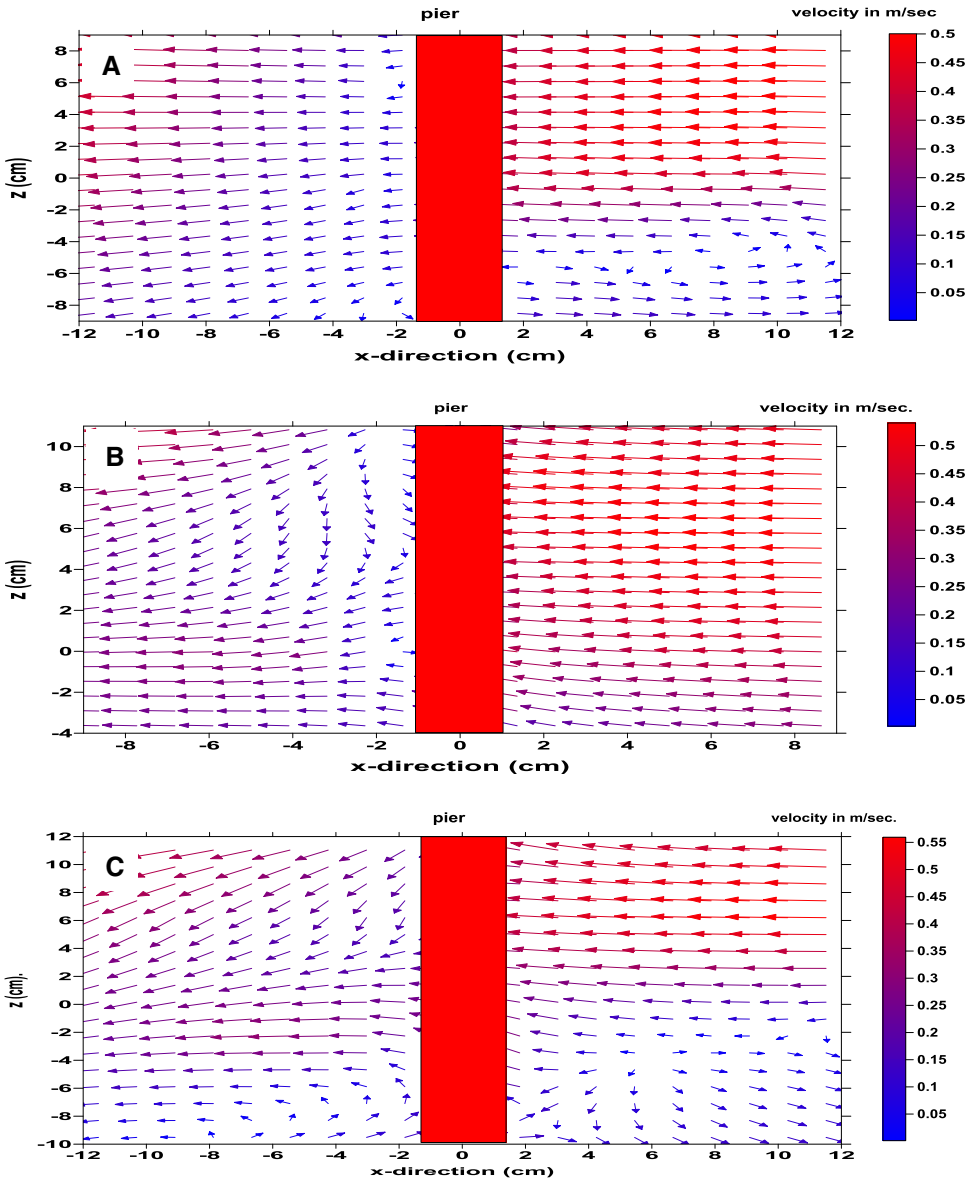

Fig. 16 Velocity vectors at vertical plane for three tested piers. **a** Upstream facing round-nosed pier, **b** downstream facing round-nosed pier and **c** circular pier

the sides of the pier, but the scour in the pier's rear was more than that of upstream facing round-nosed pier due to the separation of flow occurred with a small amount at the beginning and then increased gradually according to the shape of downstream facing round-nosed pier. In contrast, for upstream facing round-nosed pier the separation increased and then decreased, producing a little scour at the wake region.

From Fig. 16, the activity of vortices was observed (horse shoe vortex and wake vortex). At the upstream side of upstream facing round-nosed and circular piers, a strong horseshoe vortex was detected, positioned at the base of piers. In contrast, for downstream facing round-nosed pier the effect of horseshoe vortex reduced (not so visible) due to the down flow being deflected away from the base of opposite pier. It was seen from Fig. 16 that a strong wake vortex was visible and leading into scour hole in the wake region of circular and downstream facing round-nosed piers.

8 Conclusion

This paper experimentally examined the application of a new method of placing the pier in the opposite direction of flow to reduce local scour on bridge pier. Changing the position of pier is not only effective for reducing scour but it is also much more economic when it is compared with countermeasure techniques like riprap and slot.

This experimental study was conducted in order to assess the reduction of local scour around (upstream facing round-nosed, downstream facing round-nosed and circular bridge

piers). The results of comparison between the performances of bridge piers under different conditions reveal that downstream facing round-nosed bridge pier is an effective countermeasure to reduce the depth of scour.

Downstream facing round-nosed pier reduces scour depth, length of scour hole and scour hole width more than upstream facing round-nosed and circular bridge piers.

The present experimental study shows that round-nosed bridge pier performance is improved by locating it as downstream facing to the flow. We hope that the results of the present study will be benefitted by the designers and engineers.

Acknowledgments This work was supported by TUBITAK (The Scientific and Technological Research Council of Turkey). Grant 112M269.

References

1. Abed, L.; Gasser, M.M.: Model study of local scour downstream bridge piers. Proceedings national conference on hydraulic engineering, San Francisco, pp. 1738–1743 (1993)
2. Dey, S.; Raikar, R.V.: Characteristics of horseshoe vortex in developing scour holes at piers. J. Hydraul. Eng. ASCE **133**(4), 399–413 (2007)
3. Ataie-Ashtiani, B.; Aslani-Kordkandi, A.: Flow field side-by-side piers with and without scour hole. Eur. J. Mech. B/Fluids **36**, 152–166 (2012)
4. Roulund, A.; Sumer, B.M.; Fredsøe, J.; Michelsen, J.: Numerical and experimental investigation of flow and scour around a circular pier. J. Fluid Mech. **534**, 351–401 (2005)
5. Guemou, et al.: Numerical investigations of the bridge pier shape influence on the bed shear. Academic Center of Ain Temouchent, Algeria, vol. 18, Bund. Y. 5686 (2013)
6. Tafarojnoruz, A.; Gaudio, R.; Dey, S.: Flow-altering countermeasures against scour at bridge piers: review. J. Hydraul. Res. **48**(4), 441–452 (2010a)
7. Muzzammil, M.; Gangadharaiah, T.; Gupta, A.K.: An experimental investigation of a horseshoe vortex induced by a bridge pier. Water Manag. **157**, 109–119 (2004)
8. Tafarojnoruz, A.; Gaudio, R.; Calomino, F.: Evaluation of flow-altering countermeasures against bridge pier scour. J. Hydraul. Eng. **138**, 297–305 (2012)
9. Chen, S.C.; Chan H.C.; Wu, T.Y.: Experimental investigation of the Flow Field around a Bridge Pier with Hooked collar". ICSE6 Paris—August 27–31 (2012)
10. Khwairakpam, P.; Rray, S.S.; Das, S.; Das, R.; Mazumdar, A.: Scour hole characteristics around a vertical pier under clear water scour conditions. ARPN J. Eng. Appl. Sci. **7**(6), 649–654 (2012)
11. Richardson, J.R.; York, K.: Hydrodynamic countermeasures for local pier scour. J. Transp. Res. Board, TRB, no. 1375, Washington DC, pp. 186–192 (1999)
12. Ghiassi, R.; Abbasnia, A.: Investigation of vorticity effects on local scouring. Arab. J. Sci. Eng. **38**, 537–548 (2013)
13. Vaghefi, M.; Ahmadi, A.; Faraji, B.: The effect of support structure on flow patterns around T-shape spur dike in 90° bend channel. Arab. J. Sci. Eng. (2015). doi:10.1007/s13369-015-1604-2
14. Tuna, C.; Emiroglu, E.: Effect of step geometry on local scour downstream of stepped chutes. Arab. J. Sci. Eng. **38**, 579–588 (2013)
15. Onen, F.: Prediction of scour at a side-weir with GEP, ANN and regression models. Arab. J. Sci. Eng. **39**, 6031–6041 (2014)
16. Chiew, Y.M.: Scour and Scour Countermeasures at Bridge Sites. Trans. Tianjin Univ. **14**, 289–295 (2008)
17. Grimaldi, C.; Gaudio, R.; Calomino, F.; Cardoso, A.H.: Control of scour at bridge piers by a downstream bed sill. J. Hydraulic. Eng. **135**(1), 13–21 (2009)
18. Rambabu, M.; Rao, S.N.; Sundar, V.: Current-induced scour around a vertical pile in cohesive soil. In: Ocean Engineering, vol. **30**, Issue 7, Elsevier Science B.V., Amsterdam, The Netherlands, pp. 893–920 (2003)
19. Richardson, E.V.; Davis, S.R.: Evaluating Scour At Bridges Fourth Edition, U.S. Department of Transportation, Federal Highway Administration, and Washington DC, USA (2001)
20. Melville, B.W.; Chiew, Y.M.: Time scale for local scour at bridge piers. J. Hydraul. Eng. ASCE **125**(1), 59–65 (1999)